HHS Public Access

Author manuscript

J Immunol. Author manuscript; available in PMC 2016 July 15.

Published in final edited form as:

J Immunol. 2015 July 15; 195(2): 576–586. doi:10.4049/jimmunol.1500458.

Nonclassical MHC-restricted invariant Vα6 T cells are critical for efficient early innate anti-viral immunity in the amphibian *X. laevis*[1]

Eva-Stina Edholm[a], **Leon Grayfer**[a], **Francisco De Jesús**[a], and **Jacques Robert**[a,*]

[a]Department of Microbiology and Immunology, University of Rochester Medical Center, Rochester, USA

Abstract

Nonclassical MHC class Ib (class Ib)-restricted invariant T (iT) cell subsets are attracting interest because of their potential to regulate immune responses against various pathogens. The biological relevance and evolutionary conservation of iT cells has recently been strengthened by the identification of iT cells (iVα6) restricted by the class Ib molecule XNC10 in the amphibian *Xenopus laevis*. These iVα6 T cells are functionally similar to mammalian CD1d-restricted iNKT cells. Using the amphibian pathogen frog virus 3 (FV3) in combination with XNC10 tetramers and RNAi loss-of-function by transgenesis, we show that XNC10-restricted iVα6 T cells are critical for early antiviral immunity in adult *X. laevis*. Within hours following intraperitoneal FV3 infection, iVα6 T cells were specifically recruited from the spleen into the peritoneum. XNC10-deficiency and concomitant lack of iVα6 T cells resulted in less effective antiviral and macrophage antimicrobial responses, which lead to impaired viral clearance, increased viral dissemination and more pronounced FV3-induced kidney damage. Together, these findings imply that *X. laevis* XNC10-restricted iVα6 T cells play important roles in the early anti-FV3 response and that, as has been suggested for mammalian iNKT cells, they may serve as immune regulators polarizing macrophage effector functions towards more effective antiviral states.

Keywords

Invariant T cells; iT; iVα6 T cells; nonclassical MHC; X. *laevis* nonclassical MHC; XNC10; FV3; frog virus 3; amphibian; evolution; X. *laevis*

INTRODUCTION

Human and murine nonclassical MHC class Ib restricted invariant T (iT) cell subsets, such as CD1d-restricted invariant natural killer T (iNKT) and MR1-restricted mucosal-associated invariant T (MAIT) cells are being increasingly appreciated as early innate-like responders and immune regulators (1–4). For example, MAIT cells have antimicrobial activity and respond in an MR1-dependent manner to different microbes consistent with their

[1]This research was supported by National Institutes of Health, R24-AI-059830, National Sciences Foundation IOS-1456213 and Kesel Fund Award 20115123 (to E.-S.E.). L.G. was supported by a LSRF PDF from the Howard Hughes Medical Institute.

*Jacques_Robert@urmc.rochester.edu.

involvement at early stages of microbial infections (5). Similarly, iNKT cells have been associated with early stages of immune responses against diseases caused by a variety of bacterial, parasitic and viral pathogens (reviewed in (6)). With regard to viral infections, multiple lines of evidence suggest that iNKT cells are involved in immune surveillance and early clearance of different viruses including herpes simplex virus-1 (HSV-1;(7)), hepatitis B virus (HBV; (8)), and influenza A virus (IAV; (9)). In further support of the importance of these cells in anti-viral immunity, HIV-1 (10–12), HSV (13), Karposi's sarcoma-associated herpes virus (KSHV; (14)), vesicular stomatitis (VSS) and vaccinia virus (VV) (15) have all developed strategies to interfere with various stages of CD1d intracellular trafficking, thereby evading recognition by iNKT cells (reviewed in (16)). However, despite recent progress in the characterization of human and mouse iT cells, the general relevance of these cells in host defenses and the mechanisms by which iT cells respond to infections still remains poorly understood.

The evolutionary ancestry of iT cells was recently unveiled by the identification of a distinct iT cell subset in the amphibian *X. laevis*, providing compelling evidence of the biological importance of class Ib-restricted iT cells throughout jawed vertebrates (17). Similar to their mammalian counterparts, *X. laevis* iT cells (iVα6 T cells) express a unique semi-invariant T cell receptor (TCR) comprised of an invariant TCRα chain (Vα6-Jα1.43) in conjunction with a limited TCRβ repertoire. These iVα6T cells represent a significant fraction of splenic lymphocytes in healthy *X. laevis* adults (~4%) and tadpoles (~2%). In addition to the more extensively characterized iVα6 T cells *X. laevis* also posses a population of XNC10-reactive $CD8^{dim+}$ T cells with a more diverse, albeit iVα6-Jα1.43 biased TCR repertoire termed XNC10-restricted type II cells. Currently, it is unclear whether these non-invariant type II cells represent a distinct T cell subset reminiscent of mammalian type II NKT cells that are (like the type I iNKT) CD1d-restricted but do not express the canonical TCR α-chain (18). Reminiscent of CD1d requirement for the development and function of iNKT cells and MR1 for MAIT cells (2, 4), iVα6 T cells require the X. *laevis* nonclassical gene 10, (XNC10) for their development (17). Unlike most nonclassical MHC genes, XNC10 has remained highly conserved among divergent *Xenopus* species implying an important and non-redundant function for this gene (19, 20). Indeed, XNC10-deficient transgenic tadpoles lacking iVα6 T cells are more susceptible to infection with the ranavirus frog virus 3 (FV3), an ecologically relevant amphibian pathogen causing extensive disease and mortalities of wild and cultured amphibian species (21). Specifically, the defect in iVα6 T cell development resulted in dramatically higher mortality within the first weeks of infection. This critical involvement of iVα6 T cells during early anti-viral immunity in tadpoles implies that despite a long evolutionary interlude, important and specialized iT cell functions have been conserved (17).

The immune system is overall remarkably well conserved between mammals and *Xenopus*. However, unlike mammals *X. laevis* T-cell development and differentiation are subjected to an additional developmental program during metamorphosis, resulting in a adult-type immune system distinct from that of tadpoles (22). Notably, although both tadpoles and adults are immunocompetent and have conventional $CD8^{+}$ T cells and unconventional iVα6 T cells tadpoles lack significant class Ia protein expression until metamorphosis (23–25). In the context of FV3 infection, tadpoles exhibit delayed anti-FV3 innate immune responses of

lower magnitude compared to adults and typically succumb to infection (26). Conversely, despite incurring greater viral loads compared to tadpoles (27) adults are inherently more resistant to FV3 infection and mount effective anti-FV3 responses. The anti-viral response is initiated by a robust recruitment of mononuclear and polymorphonuclear phagocytes to the peritoneal cavity as early as 1 day post-infection (dpi) followed by an increase in NK cells at 3 dpi (28) culminating in $CD8^+$ T cell mediated viral clearance (28–29) and reviewed in (21). Recent findings indicate that macrophage lineage cells are integral to amphibian anti-viral immunity against FV3. Indeed peritoneal macrophages elicited with interleukin-34 (IL-34) are more resistant to *in vitro* FV3 infections compared to macrophage colony stimulating factor (MCSF)-elicited peritoneal macrophages. IL-34-derived macrophages also exhibited stronger type I interferon (IFN) gene expression response (30). These data indicate that the two macrophage growth factors polarize peritoneal macrophages for divergent roles (30).

Thus *X. laevis* provides an attractive platform to study iVαT cell involvement in a naturally occurring sublethal infection model as well as a powerful comparative model system to gather insight from an evolutionary perspective of how class Ib-mediated iT cell biology is regulated in response to viral infections.

Materials and Methods

Experimental Animals

Outbreed and LG-15 strains of *X. laevis* were from the *X. laevis* Research Resource for Immunology at the University of Rochester (http://www.urmc.rochester.edu/smd/mbi/xenopus/index.htm). Transgenic X. *laevis* was generated using I-SecI meganuclease as previously described (31). Briefly, the I-SecI-*X. laevis* nonclassical gene 10 (XNC10) shRNA-GFP expression vector was constructed by cloning the GFP reporter flanked by the 18-bp I-SecI recognition sites into the I-SceIpBSIISk+ vector (provided by R. Grainger, University of Virginia, Charlottesville, VA). Subsequently, the XNC10 shRNA under the control of the hU6 Pol III promoter was cloned into the ISecI-GFP vector. Before microinjection, X. *laevis* females were primed with human chronic gonadotropin (Sigma), and eggs were fertilized, dejellied, and injected with 80 pg I-SceI meganuclease digested XNC10shRNA-GFP expression vector as previously described (31). After injection, all embryos were incubated at 13 °C for 4 hours to delay cell division, transferred to 0.3 × modified Barth's saline supplemented with 5 μg/mL gentamicin, and reared at 18 °C until hatching. Transgenic larvae were screened for GFP expression at developmental stage 56 (32) using an SMZ1500 Nikon stereomicroscope. All animals were handled under strict laboratory and University Committee on Animal Resources regulations (100577/2003–151), and discomfort was minimized at all times.

Flow cytometry analysis

All anti-*X. laevis* mAbs were from the *X. laevis* Research Resource (https://www.urmc.rochester.edu/mbi/resources/Xenopus/). XNC10-Tetramers were generated as previously described (17). Briefly, beta 2 microglobulin (b2m) was linked via a 23-aa Gly rich C-terminal flexible linker to α1-α3 domains of XNC10 containing a BirA site-specific

biotinylation site at the end of the α3 domain and cloned into the pMIBV5-HisA expression vector (Invitrogen). The b2m-linker-XNC10 construct was expressed in Sf9 insect cells and monomeric b2m-linker-XNC10 was purified by Ni-NTA-Agarose Chromatography (Qiagen) and concentrated to 1 μg/μL using Amicon Ultra Centrifugal Filter (Millipore). BirA enzymatic biotinylation was performed for 18 h at 30 °C according to the manufacturer's protocol (Avidity), and the purified biotinylated proteins were extensively dialyzed against amphibian PBS, pH 7.5, to remove any unbound biotin. XNC10 tetramers (XNC10-T) were generated by incubating b2m-linker-XNC10 with fluorochrome-labeled streptavidin at a 5:1 ratio at room temperature for 4 hours before use in flow cytometry analysis. For detection of XNC10-T^+ cells 0.25×10^6 peritoneal leucocytes or splenocytes were stained with 5 μg XNC10-T-allophycocyanin (APC) for 30 min at 4 °C followed by incubation with X. *laevis* anti-CD8 (AM22) and FITC-conjugated goat anti-mouse secondary Abs (Southern Biotech). For analysis of peritoneal leukocytes, cells were isolated by peritoneal lavage and 0.25×10^6 cells were stained using *Xenopus* anti-CD8 (AM22), MHC class II (AM20) or MHC class I (TB17) mAbs followed by APC-conjugated goat anti-mouse secondary Abs (Southern Biotech). Dead cells were excluded using Propidium iodide (BD Pharmingen) and 50,000 events were collected with BD Accuri C6 (BD Bioscience) and analyzed using FlowJo software (Tree Star Inc.). Two-color (CD8 and XNC10-T) cell sorting by flow cytometry was performed with peritoneal leucocytes from FV3 infected animals and splenocytes from uninfected animals using a F-Aria-18 (BD Bioscience).

qPCR and genomic PCR

RNA and genomic DNA was prepared using TRIzol Reagent (Invitrogen), RNA was further treated with DNase (Ambion; Life Technologies) according to the manufacturer's protocol; 1μg total RNA was transcribed into cDNA with iScript reverse transcriptase using oligo-dT primers (Bio-Rad). Quantitative PCR parameters were: 2 min at 95 °C followed by 40 cycles of 95 °C for 15 s and 60 °C for 1 min. Relative qPCR gene expression analysis (XNC10, iVα45-Jα1.14, iVα41-Jα1.40, iVα40-Jα1.22, iVα23-Jα1.3, iVα22-Jα1.32, iVα6-Jα1.43, GCSF-R, M-CSFR, M-CSF, IL-34, iNOS, type I INF, TNFα, IL-1β, IL-10 and vDNA pol II) were performed using the ΔΔCT method. Expression of the different genes were examined relative to the endogenous GAPDH control and normalized against the lowest observed tissue expression. Absolute qPCR was performed to measure FV3 viral loads in isolated genomic DNA, using a serially diluted standard curve as previously described (27). Experiments were performed using the ABI 7300 real-time PCR system and PerfectaCTa SYBR Green FastMix, ROX (Quanta Bioscience). Expression analysis was performed using ABI Sequence Detection System software. Rearrangements of specific TCR Vα and Jα genes in the genome were detected by PCR using 50 ng genomic DNA and primers specific for iVα41-Jα1.40, iVα6-Jα1.43 and EF1-α. PCR parameters were: 5 min at 95°C followed by 40 cycles of 95°C for 30 s, 58°C for 40 s and 72°C for 1 min followed by a final extension at 72°C. All primers were validated prior to use. Primer sequences are available upon request from the *X. laevis* Research Resource (https://www.urmc.rochester.edu/mbi/resources/Xenopus/).

FV3 infections, plaque assays and histology

FV3 (*Iridoviridae*) was grown as previously described. Briefly, FV3 was grown by a single passage on BHK cells, purified by ultracentrifugation on a 30% sucrose cushion and quantified by plaque assay on a BHK cell monolayer under a 1% methylcellulose overlay (28). All infections were performed by intraperitoneal (i.p) injection of 1×10^6 plaque forming units (PFUs) of FV3 in 100μl APBS. At indicated times peritoneal leukocytes were collected by peritoneal lavage, alternatively animals were euthanized by immersion in 0.5% tricane methane sulfonate (MS-222) and tissues were removed and processed for RNA and DNA isolations. Kidneys to be assessed for infectious FV3 loads were homogenized and subjected to three rounds of freeze/thaw lysis. All plaque assays were performed on BHK cell monolayers under a 1% methylcellulose overlay, as previously described (28). For histological analysis, kidneys were isolated, immersed in 8% sucrose for 16h at 4 °C, embedded in Tissue-Tek Optimal Cutting Temperature (OCT), frozen on dry ice, sectioned (5μm sections) and hematoxylin-eosin stained. The resulting slides were examined using a Nikon Eclipse E200 phase contrast microscope, and images were taken using Nikon SPOT Idea digital camera and analyzed using SPOT Imaging software.

Statistical analysis

All quantitative data were analyzed by a one-way test of variance (ANOVA) and the Vassar Stat software (http://faculty.vassar.edu/lowry//anovalu.html) A probability level of >0.05 was considered significant.

RESULTS

Changes in frequency and tissue localization of XNC10-restricted iVα6 T cells during FV3 challenge

Intraperitoneal infection of X. *laevis* adults with the natural amphibian ranavirus pathogen Frog Virus 3 (FV3) elicits a step-wise anti-viral immune response involving both innate and adaptive immune effector cells (28, 29). To delineate the involvement of unconventional class Ib restricted iT cells during FV3 infection in MHC class Ia competent adult *X. laevis*, we sought to examine changes in location and frequency of XNC10-restricted iT cells using XNC10 tetramers (XNC10-T) (17). Given that mammalian iT cells often have specialized functions early in immune responses, we anticipated that upon FV3 infection *Xenopus* iVαT cell would be recruited to the site of inoculation prior to the influx of NK and conventional T cells. Accordingly, we intraperitoneally infected adult *Xenopus* with FV3. At different time post-infection (0, 6, 24 and 72 hours post infection [hpi]), we then determined the frequency and number of XNC10-T^+ cells in the spleen (the central amphibian draining lymphoid organ) and in peritoneal leucocytes (the first cells to come in contact with the virus) (Fig 1). Prior to FV3 infection, XNC10-restricted iVα6 T cells were principally located in the spleen where they represented on average 4% of the total lymphocyte population (Fig 1D). No XNC10-T^+ cells were detected in peritoneal leukocytes isolated from uninfected animals (Fig 1A). Comparably, flow cytometry analysis of peritoneal leukocytes revealed a significant increase in the relative fraction of XNC10-T^+ cells (1.3% ± 0.2) at 24 but not 72 hpi, which could suggest that once recruited to the infection site these cells undergo activation induced cell death or alternatively down regulated their TCRs.

Interestingly, we observed a concomitant, albeit not statistically significant decrease in the total number of splenic XNC10-T$^+$ cells as early as 6 hpi, consistent with the rapid mobilization and recruitment of XNC10-restricted iVα6 T cells to other tissues, including the peritoneal cavity, within hours following FV3 infection (Fig 1C and D). XNC10-T$^+$ cells detected in the peritoneal cavity following FV3 infection were uniformly CD8^{neg}, CD5^{neg} and MHC class II^{low+} (data not shown), corresponding to the Type I iVα6 T cell subset previously reported (17). In contrast, both type I and type II XNC10-T$^+$ cells were detected in the spleen of the same animal (1.47% ± 1.10 for type I CD8^{neg}/XNC10-T$^+$ and 1.35% ± 1.227 for type II CD8^{pos}/XNC10-T$^+$). In addition, XNC10-T$^+$ cells in the peritoneal cavity showed evidence of activation with a relative size >2 times larger (as determined by forward scatter) compared to XNC10-T reactive cells isolated from the spleen (Fig 1E). To further control for the specificity of our XNC10 tetramer and the identity of XNC10-T$^+$ cells, we sorted peritoneal and splenic XNC10-T$^+$ as well as CD8$^+$ and XNC10-T$^-$/CD8$^-$ subsets from FV3 infected (24 hpi) and uninfected animals. We determined TCRα rearrangements by PCR on genomic DNA. As expected a strong canonical Vα6-Jα1.43 signal was amplified from splenic XNC10-T$^+$ cells (either CD8$^+$ or CD8^{neg}), whereas no Vα6-Jα1.43 signal was detect in XNC10-T negative cells (Fig 1B). In contrast, signal for the irrelevant TCR rearrangement Vα41-Jα1.40 was only amplified from splenic XNC10-T$^-$/CD8$^-$ cells and not from XNC10-T$^+$ cells. Importantly, XNC10-T$^+$ but not CD8$^+$ cells isolated from the peritoneal cavity were positive for the Vα6-Jα1.43 rearrangement. Interestingly, the Vα6-Jα1.43 rearrangement was also detected in a fraction of PLs from infected animals negatively stained for CD8 and XNC10-tetramer. This suggests that a fraction of iVα6 T cells infiltrating the peritoneum during infection might have down regulated their surface TCR expression.

To obtain additional evidence of the splenic egress and consequent transitory influx of iVα6T cells into the peritoneal cavity, we quantified transcript levels of the specific invariant Vα6-Jα1.43 rearrangement in the spleen, peritoneal leukocytes and kidney (the main site of FV3 replication) at different time points following FV3 infection (Fig 2A, D and G). Since iVα6 T cells interact with the class Ib molecule XNC10, we also examined its gene expression profile (Fig 2B, E and H). To evaluate viral loads and dissemination we determined the FV3 genome copy number in different tissues using absolute qPCR (Fig 2C, F and I). Consistent with the loss of splenic XNC10-T$^+$ cells following FV3 infection, expression of the iVα6-Jα1.43 transcript was markedly reduced by 1 dpi, remaining low at 3 dpi, and increasing again at 6 dpi (Fig 2A). This suggests the replenishment of the iVα6T cell pool presumably via influx of naive iVα6 T cells from the thymus. Conversely peritoneal leukocytes iVα6-Jα1.43 expression was undetectable in uninfected animals, became significantly elevated at 6 hpi, markedly peaked at 1 dpi then returned to low but detectable levels from 2 to 6 dpi, indicating a rapid and transitory influx of iVα6 T cells to the peritoneal cavity upon intraperitoneal FV3 inoculation (Fig 2D). It is to note that the increase in iVα6-Jα1.43 transcript levels observed at 6 hpi likely reflects an initial, low frequency iVα6 T cell infiltration that was below detection levels using XNC10-T-flow cytometry analysis. In kidneys, iVα6-Jα1.43 expression was modest and highly variable, with no significant increase in iVα6-Jα1.43 mRNA levels until 6 dpi (Fig 2G). As expected, high viral loads were detected in peritoneal leucocytes as early as 6 hpi, whereas splenic

FV3 loads were either undetected or modest with an average of 2 logs lower viral loads than in peritoneal leucocytes (Fig 2F, C). Congruent with the kidney being the main site of FV3 replication, viral loads in this tissue were higher and increased from 1 to 3 dpi, followed by a decline at 6 dpi consistent with the previously described influx of $CD8^+$ T cells and the onset of viral clearance (29).

During the course of infection, the most dramatic change in XNC10 gene expression was observed in peritoneal leukocytes. Notably, unlike spleen that exhibited high and uniform expression levels regardless of FV3 infection, XNC10 gene expression in peritoneal leukocytes was markedly induced upon FV3 infection with a significant increase detected as early as 6 hpi followed by a peak at 2 dpi (Fig 2B, E). In kidneys, XNC10 gene expression was delayed and modest compared to peritoneal leukocytes; it did not significantly increase until 2 dpi, remaining elevated at 3 dpi and then diminishing by 6 dpi (Fig 2H). Collectively, these data indicate that XNC10-restricted iVα6 T cells are rapidly mobilized upon FV3 infection, leaving the spleen and migrating to the peritoneal cavity several days prior to the influx of NK and conventional T cells.

Relative expression of other putative invariant TCRα gene rearrangements in response to FV3 infection

Although the antigen(s) recognized by iVα6 T cells has not yet been identified, we sought to determine whether the influx of iVα6T into the peritoneal cavity following FV3 infection reflected the recruitment of only this particular iT cell subset. Accordingly, we determined the mRNA levels of the five additional predominant putative iTCRα rearrangements previously identified (Vα45-Jα1.14, Vα41-Jα1.40, Vα40-Jα1.22, Vα23-Jα1.3Vα22-Jα1.32 and iVα6-Jα1.43 (17) in peritoneal leukocytes following FV3 infection (Fig 3A). Remarkably, iVα6-Jα1.43 was the only rearrangement that was significantly elevated in expression upon FV3 infection, which indicates a specific recruitment of iVα6T cells in response to FV3 challenge. We also noted a relative decrease in the expression of the Vα41-Jα1.40 rearrangement post-FV3 infection, suggesting that the particular iT cell subset expressing this rearrangement is predominant in the peritoneal cavity in naive animals. It is noteworthy that no significant increase in gene expression in any of the six iTCRα rearrangements, including the iVα6-Jα1.43, was observed following intraperitoneal challenge with heat-killed *E. coli* (Fig 3B). This type of bacterial stimulation has been shown to induce a strong non-specific inflammatory response accompanied by a robust recruitment and accumulation of innate leukocytes in the peritoneal cavity (28). These results argue against a general infiltration of iT cells due to inflammation and provide compelling evidence that iVα6 T are specifically recruited to the initial site of FV3 infection.

XNC10 loss-of-function by RNAi *in vivo* results in compromised viral clearance in the peritoneal cavity

Based on our results indicating that iVα6 T cells are rapidly (within hours) recruited to the peritoneal cavity upon FV3 infection, we hypothesized that these cells are critical for eliciting an efficient antiviral immune response. As such, we anticipated that iVα6 T cell deficiency would results in weakened host resistance to FV3. To address this hypothesis, we

utilized a XNC10 loss-of-function approach shown to result in impaired iVα6 T cell development (17, 31). One year-old F0 animals deficient for XNC10 were generated by combining RNA interference with I-SecI meganuclease-mediated transgenesis. Transgenic and age matched control animals (reared from fertilized eggs of the same batch that were dejellied but not injected with the XNC10shRNA) were intraperitoneally infected with FV3 and levels of XNC10 knockdown in the spleen was assessed by qPCR at 6 dpi. Only transgenic animals that showed a >75% XNC10 knock-down (n=5) compared to the average XNC10 gene expression in control animals (n=10, Fig 4A) were used in further analysis.

Consistent with our published data (17), XNC10 silencing in transgenic animals resulted in a drastically decreased expression of the invariant Vα6-Jα1.43 rearrangement in the spleen (P = 0.00655) compared with age-matched controls (Fig 4B). Upon FV3 infection, the sharp increase of both XNC10 and iVα6-Jα1.43 transcript levels observed at 1 dpi in peritoneal leukocytes of control animals was ablated in transgenic animals (Fig 4C and D). Importantly, XNC10 and iVα6 T cell deficiency impacted FV3 viral replication, as evidenced by significantly higher viral loads in transgenic animals at both 1 dpi (P = 0.01903) and 6 dpi (P = 0.02332) compared to control animals (Fig 4C). Moreover, 7 out of 10 control *X. laevis* displayed 1–2 log units lower FV3 loads on day 6 compared to day 1 post infection indicative of onset of viral clearance. In contrast, the transgenic animals displayed either the same (3/5) or even 1 log higher (2/5) viral loads at 6 dpi compared to 1 dpi further suggesting that XNC10-deficient transgenic *X. laevis* have an impaired ability to control FV3 replication.

XNC10-deficiency has little effect on the overall recruitment of leukocytes into the peritoneal cavity following FV3 infection

To assess for possible difference in the peritoneal leukocytes composition resulting from XNC10-deficiency, we performed flow cytometry analysis with XNC10-deficient transgenic and genetically identical non-transgenic isogenetic LG-15 cloned animals with a defined MHC a/c haplotype. In several independent experiments (one representative shown in Fig 5), we found comparable compositions of MHC class II and MHC class I surface positive cells in uninfected animals as well as similar frequencies of $CD8^+$ T cell (Fig 5A). Moreover, both control and XNC10-deficient transgenic animals showed a robust influx of large, highly internally complex MHC class II^{low} staining cells at 1 dpi with overall similar MHC class II mean fluorescent intensity, 1002± 275 for transgenic and 724± 58 for control animals. (Fig 5B). We noted, however, that peritoneal leukocytes isolated from infected XNC10-deficient transgenic animals consistently contained a population of small, agranular MHC class II^{low} staining cells (indicated by arrow) constituting between 9–11% of the total population that was absent in control animals (Fig 5B).

Effects of XNC10-deficiency and lack of iVα6 cells on antiviral peritoneal leukocyte response

To delineate the putative functional roles of XNC10-restricted iVα6 T cells during FV3 infection, we examined peritoneal leukocytes isolated at the peak of iVα6T cell infiltration (1 dpi) and at the peak of the conventional $CD8^+$ T cell response (6 dpi, (25, 27)). Although the total number of leukocyte infiltrating the peritoneum at 1 dpi was slightly decreased in

infected XNC10-deficient transgenic animals compared to infected controls, it was not statistically significant (Fig 6A). Using granulocyte colony stimulating factor receptor (GCSF-R) and macrophage colony-stimulating factor receptor (MCSF-R) gene expression determined by qPCR to monitor polymorphonuclear granulocytes and mononuclear phagocytes, we observed similar gene response kinetics in control and transgenic animals. There was a similar early increase of GCSF-R at 1 dpi and a later increase of MCSF-R at 6 dpi in both peritoneal leukocyte of control and XNC10-deficient transgenics consistent with an early infiltration of polymorphonuclear granulocytes followed by an influx of mononuclear phagocytes (Fig 6A–C). We have previously shown that *X. laevis* macrophage-lineage cells are integral to immune responses against FV3 (33) (34) and that the two macrophage growth factors, MCSF (35) and IL-34 (30) elicit distinct macrophage effector functions (30). In particular, IL-34 derived peritoneal macrophages exhibit a more robust type I IFN and iNOS expression responses, and more potent anti-FV3 activity. Therefore, we sought to determine whether part of the delayed anti-FV3 immune response in XNC10 loss-of-function and lack of iVα6 T cells could reflect a change in macrophage effector functions. To address this possibility, we monitored the expression profiles of MCSF, IL-34 and inducible nitric oxide synthase (iNOS) genes in peritoneal leukocytes isolated from uninfected, 1 dpi (early innate response) and 6 dpi (peak of conventional $CD8^+$ T cell response) XNC10-deficient transgenic and control X. *laevis.* Notably, the early infiltration and accumulation of leukocytes at 1 dpi in XNC10-deficient transgenic animals was accompanied by significantly lower gene expression for IL-34 but not MCSF (Fig 6D, E and F). In addition, the iNOS gene expression response was delayed in FV3-infected XNC10 deficient transgenic animal and significantly increased only at 6 dpi in contrast to 1 dpi in control animals. This suggest that iVα6 T cells have a notable role in promoting macrophage antimicrobial immunity.

Given that type I IFN in *X. laevis* as in mammals is critical in controlling viral replication (27), we postulated that the delayed IL-34 gene expression upon FV3 infection in peritoneal leukocytes of XNC10-deficient animals should impact type I IFN gene expression. Indeed unlike control animals, type I IFN gene expression was magnitudes lower at 1 dpi in peritoneal leukocytes of XNC10-deficient animals, whereas at 6 dpi both control and transgenic animals exhibited high transcript levels of type I IFN (Fig 7A). The defect in anti-viral gene expression response in transgenic animals was not general since FV3 infection induced similar expression profiles for the pro-inflammatory gene IL-1β (28) and the anti-inflammatory gene IL10 between control and XNC10-deficient animals. Notably, the TNFα expression remained elevated at 6 dpi in transgenic animals, correlating with the higher viral loads observed in these animals (Fig 7B, C and D). Overall these findings suggest that XNC10-deficient transgenic animals lacking iVα6 T cells mount delayed anti-FV3 responses that is in part resulting from a defect in macrophage effector functions.

Effects of XNC10-deficiency and lack of iVα6 cells on viral replication and pathogenesis in kidneys

Given our findings that the onset of type I INF anti-viral response was delayed in peritoneal leukocytes of XNC10-deficient transgenic animals, we next examined the impact of this deficiency on viral replication and pathogenesis in the kidneys, the main site of FV3

replication. Notably, kidneys isolated from XNC10-deficient transgenic animals showed significantly higher FV3 genome copy numbers compared to controls as assessed by qPCR detecting the FV3 vDNA Pol II gene (Fig 8A, $P = 0.05$). Furthermore, compared to controls, kidney homogenates from transgenic animals contained greater levels of infectious viral particles (PFU/ml; Fig 8B, $P = 0.02543$), clearly indicating a less efficient control of viral replication. To determine whether this increased viral replication resulted in increased pathology, we conducted a histological examination of kidneys from the different treatment groups. Most strikingly, in absence of iVα T cells, we observed dramatically more pronounced tissue damages in FV3 infected kidneys compared to FV3 infected controls, including a marked loss of tissue architecture and destruction of the characteristic proximal tubular epithelia in XNC10-deficient transgenic animals (Fig 8E and F). We also assessed the degree of viral dissemination in other tissues including spleen, liver and intestine of transgenic and control *X. laevis* at 6 dpi but did not see significant difference at these secondary sites (Fig 8G–I). Collectively, our findings suggest that the loss of the class Ib MHC molecule XNC10 and the XNC10-restricted iVα6 T cell population leads to an impaired anti-FV3 response in the class Ia competent adult *X. laevis* that is in part due to less efficient anti-viral immunity and macrophage effector functions.

DISCUSSION

This study show for the first time outside mammals, the decisive role of class Ib restricted iT cells in mounting timely and efficient anti-viral immune responses. This in turn provides compelling evidence of the evolutionary conserved roles of class Ib restricted iT cells in anti-viral immunity reinforcing the biological conservation of these cells, throughout jawed vertebrates. Using a loss-of-function approach by transgenesis we showed that silencing XNC10 *in vivo* resulted in a delayed anti-viral immune response to FV3, permitting more robust viral replication and dissemination during the early phase of infection leading to increased tissue damage in the kidney. This impaired ability to control early FV3 replication in class Ia competent adults, obtained by specifically silencing a single class Ib gene, XNC10 and the correlating loss of XNC10-restricted iVα6T cells has a fundamental significance, because although the involvement of iNKT cells in response to viral infections is documented in humans and mice, the biological role(s) of this system is still not fully understood and likely highly multifaceted.

The spatial and temporal changes in iVα6 T cell frequency and numbers observed during FV3 infection are indicative of the rapid recruitment and migration of iVα6T cells from the spleen to the peritoneal cavity and later to the kidney. These changes correlate well with the dissemination of infection. The rapid decrease in iVα6 T cells and Vα6-Jα1.43 transcript levels in the spleen, which in *X. laevis*, represents both the primary and in the absence of lymph nodes the only secondary lymphoid organ, is followed by a concomitant increase in iVα6 T cells and Vα6-Jα1.43 transcript levels in peritoneal leukocytes by 1 dpi. It is noteworthy that the iVα6 T cell influx into the peritoneal cavity occurs days before the detection of NK cell infiltration (3 dpi (28)) and well before the peak of the conventional $CD8^+$ T cells response (6 dpi (29)). This strongly suggests that iVα6 T cells function as early responders and putative modulators of anti-FV3 immune responses. Although the mechanisms governing the recruitment of iVα6 T cells to the peritoneal cavity is presently

unknown, the observed increase in size and complexity of these cells between spleen and the peritoneum following FV3 infection is consistent with an activation state. It is also interesting to note that the canonical Vα6-Jα1.43 rearrangement was detected not only in sorted XNC10-T$^+$ but also in CD8/XNC10 double negative PLs from infected animals. This suggests a down regulation of the TCR for a fraction of infiltrating iVα6 T cells, which is consistent with an activation of iVα6 T cells. The absence of detectable CD8, CD5 and class II surface expression by peritoneal XNC10-T$^+$ cells strongly suggest that XNC10-restricted T cells infiltrating the peritoneal cavity following FV3 infection are predominantly, if not exclusively, type I iVα6 T cells. Although, the involvement of type II XNC10-restricted T cells expressing low level of CD8 and a more diverse, albeit iVα6-Jα1.43 biased TCR repertoire, remains possible, this subset will first need a better characterization with the help of specific reagents (e.g., Abs).

While the effector functions of iVα6 T cells is likely to be mediated by multiple mechanisms that remains to be characterized in detail, our data suggests that iVα6 T cells promote timely and effective type I IFN mediated anti-FV3 responses and influence the polarization of peritoneal macrophages into more robust anti-viral state. Infection studies in *X. laevis* and other amphibian species have shown that macrophage-lineage cells are integral to amphibian immunity against FV3 (30, 33–34). We have recently demonstrated that the two principal mediators of macrophage development, MCSF and IL-34 elicit peritoneal macrophages with distinct antiviral properties (30). Compared to MCSF-elicited peritoneal leukocytes, IL-34-derived peritoneal leukocytes were more resistant to FV3 infection *in vitro*, and exhibit more robust type I IFN and iNOS gene expression responses (30). Consistent with this notion, XNC10-deficient transgenic animals exhibited delayed IL-34, iNOS and type I IFN gene expression responses during the first stages of FV3 infection. Thus the modulation of macrophage antiviral effector functions by iT cells suggested by our findings, provides novel and promising avenues of research.

During the time span of our study XNC10-deficiency and lack of iVα6 T cells did not increase FV3 induced mortality (data not shown). However, transgenic animals displayed a weaker ability to control FV3 replication in the kidney by 6 dpi, at the peak of CD8$^+$ T cell infiltration and the onset of viral clearance, resulting in dramatic kidney pathology. While the long-term consequences of such tissue damages on survival and fitness in the wild remains to be determined, this observation reinforces the importance of a functional early iVαT cell response in the generation of appropriate anti-FV3 immune responses. Thus, our findings strongly suggest that in the context of FV3 infection XNC10 impairment results in inefficient early recruitment of iVα6 T cells to the site of infection. The absence of these iT cells in turn prevents the generation of IL-34 derived macrophages resulting in a delayed type I IFN and iNOS responses and weakened host control of FV3 replication.

In line with our study in *X. laevis*, activation of murine iNKT cells by simultaneous administration of αGalCer and infection with a mouse-adapted influenza A strain (PR8) initiated rapid recruitment of iNKT from the liver to the infected lungs, which resulted in enhanced early innate immune response, reduced viral titers in the lungs and a significantly improved disease outcome (9). Furthermore, adoptive transfer of iNKT cells rescued the survival of Jα18$^{-/-}$ mice in a high pathogenicity model of influenza infection (36). A

functional role of iNKT cells during influenza infection was suggested by the observation that iNKT cells suppress virally induced expansion of myeloid-derived suppressor cells, including immature dendritic cells, macrophages and granulocytes and reduced the suppressive activity of these cells thus restoring $CD8^+$ T cell cytotoxic responses and viral clearance (36). However, the involvement of IL-34 in this system was not investigated. In the context of hepatitis B virus (HBV) infections, α-GalCer injection profoundly inhibited HBV replication in the liver of HBV transgenic mice through activation of intrahepatic iNKT cells (8). The antiviral effects of α-GalCer were rapid (inhibition of HBV replication was detected within 24 hours post injection), mediated by IFN-γ as well as IFN-α/β and associated with a strong induction of 2'5'-OAS, iNOS and TNF-α gene expression (8). Furthermore, α-GalCer induced inhibition of HBV replication was T cell-independent, but did result in an increased infiltration of NK cells into the liver peaking at 3 days post injection suggesting that activated iNKT cells trigger the recruitment and activation of NK cells.

Although, the nature of the XNC10 ligand is presently unknown, primary and secondary sequence analysis of XNC10 and its cognate invariant TCRα receptor suggested that XNC10 presents a common or conserved antigenic motif to iVα6 T cells (17, 19, 20). In support of a specific recruitment of iVα6 T cells in response to a FV3-derived antigen presented in the context of XNC10 only the iVα6-Jα1.43 rearrangement and not the other five invariant TCRα rearrangements (17) were elevated in response to FV3 infection. Moreover, no increase in the expression of iVα6-Jα1.43 rearrangement was detected after intraperitoneal stimulation with heat-killed bacteria, arguing against a non-specific inflammation induced recruitment of iT cells. However, whether iVα6 activation during a FV3 infection result from a direct interaction with XNC10 expressing cells presenting a virus derived antigen or a endogenous ligand remains to be determined. It is to note that FV3 virions contain peptide and lipid components that could in theory be processed by $XNC10^+$ cells, loaded onto XNC10 and presented to iVα6 T cells (21). It is also possible that FV3 infection induces synthesis and/or post-translational modification of an endogenous antigen(s) or products that would enhance XNC10 surface expression thus facilitating XNC10-iVα6 TCR interaction. Alternatively, iVα6 T cell activation could be driven by cytokines produced by innate immune cells in an Ag-independent manner. For example, upon infection with mouse cytomegalovirus, iNKT cells were activated and produced IFN-γ in response to IL-12 and IFN-α/β stimulation in a CD1d independent manner (37–39).

In summary, these results provide evidence that in response to a natural viral pathogen XNC10-restricted iVα6 T cells are specifically recruited to the site of infection, become activated and by enhancing and possibly polarizing the early innate immune response such as macrophages critically contribute to antiviral immunity and improved disease outcome. This evolutionary functional conservation, highlighting the involvement of class Ib restricted iT cells in early response and immune modulation against viral challenges show the biological importance of iT cells in all jawed vertebrates. In particular the potential function of iVαT cells and possibly iNKT cells in polarizing macrophages and other leukocyte promises to be an interesting area of investigation.

ACKNOWLEDGMENTS

We thank Tina Martin for the expert animal husbandry and Maureen Banach for discussions and critical reading of the manuscript.

BIBLIOGRAPHY

1. Bendelac A, Lantz O, Quimby ME, Yewdell JW, Bennink JR, Brutkiewicz RR. CD1 recognition by mouse NK1+ T lymphocytes. Science. 1995; 268:863–865. [PubMed: 7538697]
2. Bendelac A. Positive selection of mouse NK1+ T cells by CD1-expressing cortical thymocytes. The Journal of experimental medicine. 1995; 182:2091–2096. [PubMed: 7500054]
3. Tilloy F, Treiner E, Park SH, Garcia C, Lemonnier F, de la Salle H, Bendelac A, Bonneville M, Lantz O. An invariant T cell receptor alpha chain defines a novel TAP-independent major histocompatibility complex class Ib-restricted alpha/beta T cell subpopulation in mammals. The Journal of experimental medicine. 1999; 189:1907–1921. [PubMed: 10377186]
4. Treiner E, Duban L, Bahram S, Radosavljevic M, Wanner V, Tilloy F, Affaticati P, Gilfillan S, Lantz O. Selection of evolutionarily conserved mucosal-associated invariant T cells by MR1. Nature. 2003; 422:164–169. [PubMed: 12634786]
5. Le Bourhis L, Martin E, Peguillet I, Guihot A, Froux N, Core M, Levy E, Dusseaux M, Meyssonnier V, Premel V, Ngo C, Riteau B, Duban L, Robert D, Huang S, Rottman M, Soudais C, Lantz O. Antimicrobial activity of mucosal-associated invariant T cells. Nature immunology. 2010; 11:701–708. [PubMed: 20581831]
6. Juno JA, Keynan Y, Fowke KR. Invariant NKT cells: regulation and function during viral infection. PLoS pathogens. 2012; 8:e1002838. [PubMed: 22916008]
7. Grubor-Bauk B, Simmons A, Mayrhofer G, Speck PG. Impaired clearance of herpes simplex virus type 1 from mice lacking CD1d or NKT cells expressing the semivariant V alpha 14-J alpha 281 TCR. Journal of immunology. 2003; 170:1430–1434.
8. Kakimi K, Guidotti LG, Koezuka Y, Chisari FV. Natural killer T cell activation inhibits hepatitis B virus replication in vivo. The Journal of experimental medicine. 2000; 192:921–930. [PubMed: 11015434]
9. Ho LP, Denney L, Luhn K, Teoh D, Clelland C, McMichael AJ. Activation of invariant NKT cells enhances the innate immune response and improves the disease course in influenza A virus infection. European journal of immunology. 2008; 38:1913–1922. [PubMed: 18521958]
10. Moll M, Andersson SK, Smed-Sorensen A, Sandberg JK. Inhibition of lipid antigen presentation in dendritic cells by HIV-1 Vpu interference with CD1d recycling from endosomal compartments. Blood. 2010; 116:1876–1884. [PubMed: 20530791]
11. Chen N, McCarthy C, Drakesmith H, Li D, Cerundolo V, McMichael AJ, Screaton GR, Xu XN. HIV-1 down-regulates the expression of CD1d via Nef. European journal of immunology. 2006; 36:278–286. [PubMed: 16385629]
12. Hage CA, Kohli LL, Cho S, Brutkiewicz RR, Twigg HL 3rd, Knox KS. Human immunodeficiency virus gp120 downregulates CD1d cell surface expression. Immunology letters. 2005; 98:131–135. [PubMed: 15790518]
13. Yuan W, Dasgupta A, Cresswell P. Herpes simplex virus evades natural killer T cell recognition by suppressing CD1d recycling. Nature immunology. 2006; 7:835–842. [PubMed: 16845396]
14. Sanchez DJ, Gumperz JE, Ganem D. Regulation of CD1d expression and function by a herpesvirus infection. The Journal of clinical investigation. 2005; 115:1369–1378. [PubMed: 15864354]
15. Renukaradhya GJ, Webb TJ, Khan MA, Lin YL, Du W, Gervay-Hague J, Brutkiewicz RR. Virus-induced inhibition of CD1d1-mediated antigen presentation: reciprocal regulation by p38 and ERK. Journal of immunology. 2005; 175:4301–4308.
16. Van Kaer L, Joyce S. Viral evasion of antigen presentation: not just for peptides anymore. Nature immunology. 2006; 7:795–797. [PubMed: 16855602]
17. Edholm ES, Albertorio Saez LM, Gill AL, Gill SR, Grayfer L, Haynes N, Myers JR, Robert J. Nonclassical MHC class I-dependent invariant T cells are evolutionarily conserved and prominent

from early development in amphibians. Proceedings of the National Academy of Sciences of the United States of America. 2013; 110:14342–14347. [PubMed: 23940320]

18. Behar SM, Podrebarac TA, Roy CJ, Wang CR, Brenner MB. Diverse TCRs recognize murine CD1. Journal of immunology. 1999; 162:161–167.
19. Edholm ES, Goyos A, Taran J, De Jesus Andino F, Ohta Y, Robert J. Unusual evolutionary conservation and further species-specific adaptations of a large family of nonclassical MHC class Ib genes across different degrees of genome ploidy in the amphibian subfamily Xenopodinae. Immunogenetics. 2014; 66:411–426. [PubMed: 24771209]
20. Goyos A, Sowa J, Ohta Y, Robert J. Remarkable conservation of distinct nonclassical MHC class I lineages in divergent amphibian species. Journal of immunology. 2011; 186:372–381.
21. Chinchar VG. Ranaviruses (family Iridoviridae): emerging cold-blooded killers. Archives of virology. 2002; 147:447–470. [PubMed: 11958449]
22. Robert J, Ohta Y. Comparative and developmental study of the immune system in Xenopus. Developmental dynamics : an official publication of the American Association of Anatomists. 2009; 238:1249–1270. [PubMed: 19253402]
23. Flajnik MF, Hsu E, Kaufman JF, Pasquier LD. Changes in the immune system during metamorphosis of Xenopus. Immunology today. 1987; 8:58–64. [PubMed: 25291685]
24. Flajnik MF, Kaufman JF, Hsu E, Manes M, Parisot R, Du Pasquier L. Major histocompatibility complex-encoded class I molecules are absent in immunologically competent Xenopus before metamorphosis. Journal of immunology. 1986; 137:3891–3899.
25. Salter-Cid L, Nonaka M, Flajnik MF. Expression of MHC class Ia and class Ib during ontogeny: high expression in epithelia and coregulation of class Ia and lmp7 genes. Journal of immunology. 1998; 160:2853–2861.
26. De Jesus Andino F, Chen G, Li Z, Grayfer L, Robert J. Susceptibility of Xenopus laevis tadpoles to infection by the ranavirus Frog-Virus 3 correlates with a reduced and delayed innate immune response in comparison with adult frogs. Virology. 2012; 432:435–443. [PubMed: 22819836]
27. Grayfer L, De Jesus Andino F, Robert J. The amphibian (Xenopus laevis) type I interferon response to frog virus 3: new insight into ranavirus pathogenicity. Journal of virology. 2014; 88:5766–5777. [PubMed: 24623410]
28. Morales HD, Abramowitz L, Gertz J, Sowa J, Vogel A, Robert J. Innate immune responses and permissiveness to ranavirus infection of peritoneal leukocytes in the frog Xenopus laevis. Journal of virology. 2010; 84:4912–4922. [PubMed: 20200236]
29. Morales HD, Robert J. Characterization of primary and memory CD8 T-cell responses against ranavirus (FV3) in Xenopus laevis. Journal of virology. 2007; 81:2240–2248. [PubMed: 17182687]
30. Grayfer L, Robert J. Divergent antiviral roles of amphibian (Xenopus laevis) macrophages elicited by colony-stimulating factor-1 and interleukin-34. Journal of leukocyte biology. 2014; 96:1143–1153. [PubMed: 25190077]
31. Nedelkovska H, Edholm ES, Haynes N, Robert J. Effective RNAi-mediated beta2-microglobulin loss of function by transgenesis in Xenopus laevis. Biology open. 2013; 2:335–342. [PubMed: 23519478]
32. Nieuwkoop, PD.; F, J. Normal tables of Xenopus laevis. North-Holland Amsterdam: 1967.
33. Robert J, Grayfer L, Edholm ES, Ward B, De Jesus Andino F. Inflammation-induced reactivation of the ranavirus Frog Virus 3 in asymptomatic Xenopus laevis. PloS one. 2014; 9:e112904. [PubMed: 25390636]
34. Grayfer L, Andino Fde J, Chen G, Chinchar GV, Robert J. Immune evasion strategies of ranaviruses and innate immune responses to these emerging pathogens. Viruses. 2012; 4:1075–1092. [PubMed: 22852041]
35. Grayfer L, Robert J. Colony-stimulating factor-1-responsive macrophage precursors reside in the amphibian (Xenopus laevis) bone marrow rather than the hematopoietic subcapsular liver. Journal of innate immunity. 2013; 5:531–542. [PubMed: 23485675]
36. De Santo C, Salio M, Masri SH, Lee LY, Dong T, Speak AO, Porubsky S, Booth S, Veerapen N, Besra GS, Grone HJ, Platt FM, Zambon M, Cerundolo V. Invariant NKT cells reduce the immunosuppressive activity of influenza A virus-induced myeloid-derived suppressor cells in

mice and humans. The Journal of clinical investigation. 2008; 118:4036–4048. [PubMed: 19033672]

37. Wesley JD, Tessmer MS, Chaukos D, Brossay L. NK cell-like behavior of Valpha14i NK T cells during MCMV infection. PLoS pathogens. 2008; 4:e1000106. [PubMed: 18636102]
38. Holzapfel KL, Tyznik AJ, Kronenberg M, Hogquist KA. Antigen-dependent versus -independent activation of invariant NKT cells during infection. Journal of immunology. 2014; 192:5490–5498.
39. Tyznik AJ, Tupin E, Nagarajan NA, Her MJ, Benedict CA, Kronenberg M. Cutting edge: the mechanism of invariant NKT cell responses to viral danger signals. Journal of immunology. 2008; 181:4452–4456.

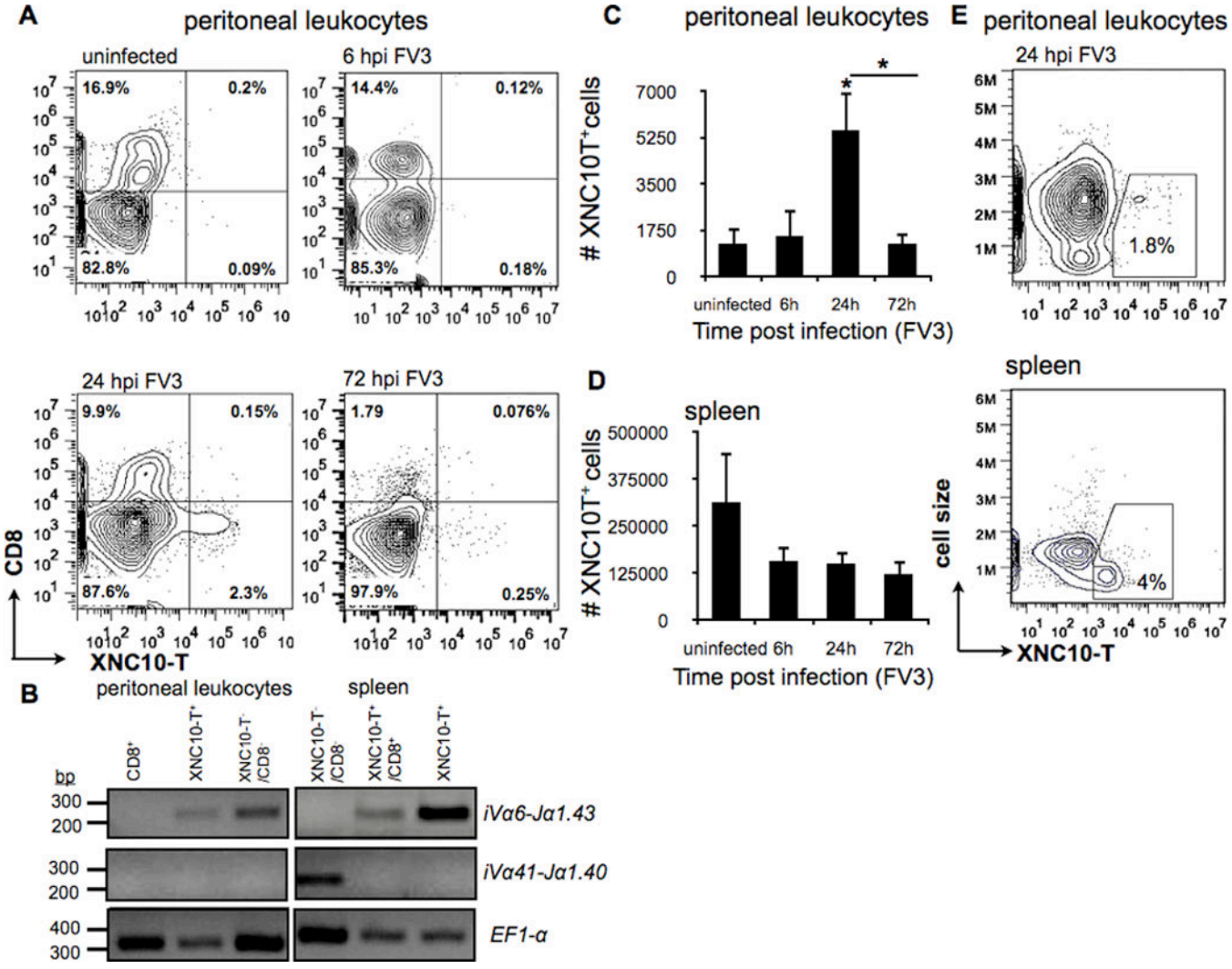

Fig. 1. Rapid egress of XNC10-restricted iVα6 T cells from the spleen to the peritoneal cavity following intraperitoneal FV3 inoculation

One-year old outbreed X. *laevis* were infected i.p. with 1×10^6 PFU of FV3, spleen and peritoneal leukocytes were collected at indicated times and analyzed by flow cytometry. (A) Representative flow cytometry of live peritoneal leukocytes isolated by peritoneal lavage from either uninfected or i.p. FV3 infected adults at 6, 24 and 72 hpi and double stained with XNC10-T and anti-CD8 mAb. (B) Rearrangement of specific TCR Vα and Jα genes in the genome of sorted cells from either uninfected spleen of peritoneal leukocytes isolated by peritoneal lavage from FV3 infected adults at 24 hpi. PCR was performed on 50 ng genomic DNA (40 cycles) using primers specific for iVα41-Jα1.40, iVα6-Jα1.43 and Ef1-α Total number of live XNC10-T^+ staining cells from either (C) peritoneal leukocytes or (D) spleen leucocytes collected at indicated times. Data are means (± SE) of seven individuals/indicated time point (n=7). *$P < 0.05$ above bars denotes statistical significance relative to respective uninfected controls and *$P < 0.05$ above the line denote significant differences between the indicated groups (Student t test). (E) Representative flow cytometry analysis showing

forward scatter versus XNC10-T staining for spleen leukocytes and peritoneal leucocytes isolated from either a uninfected frog or 24 hours following FV3 infection respectively.

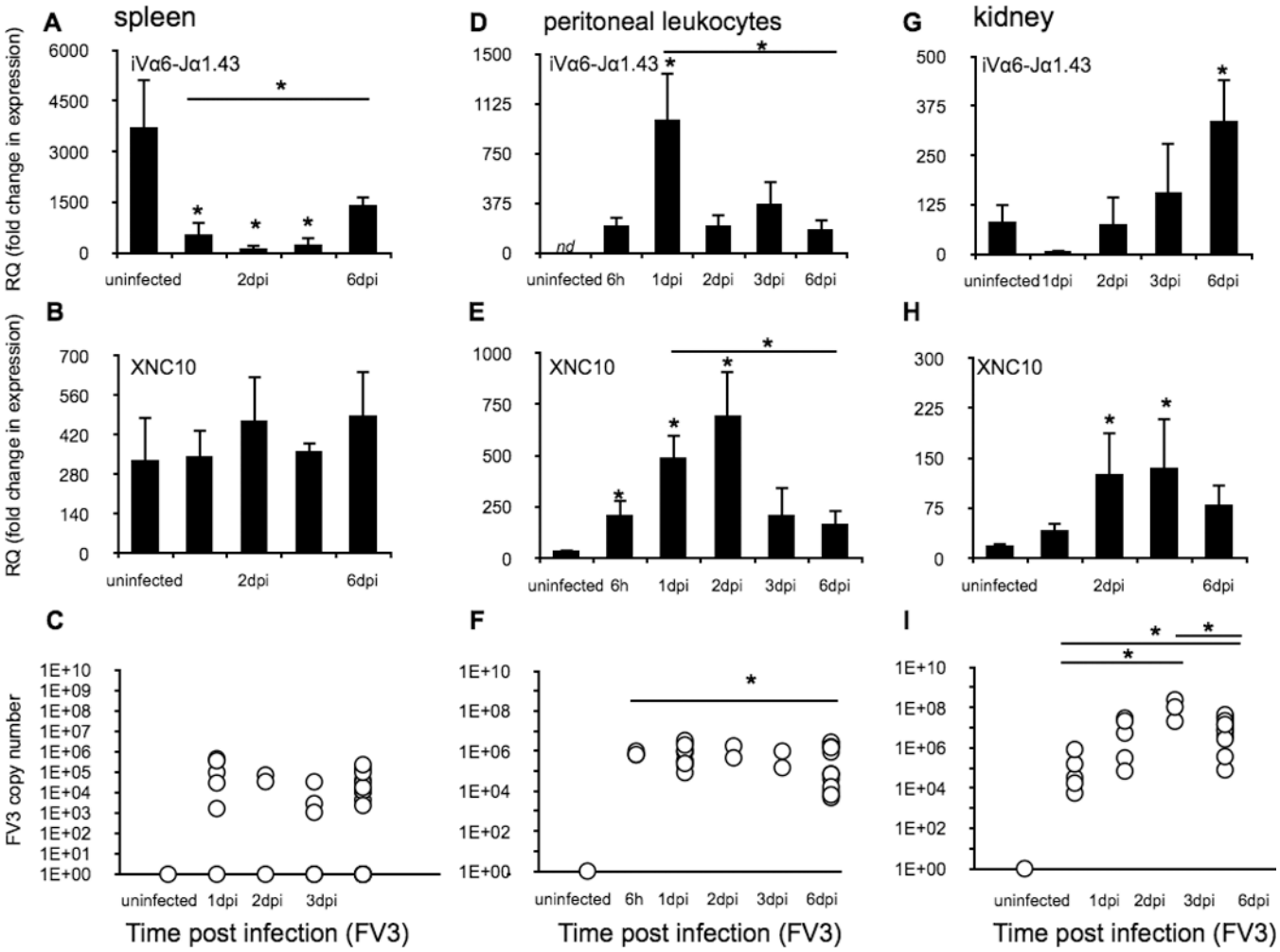

Fig. 2. Tissue-specific XNC10 and iVα6-Jα1.43 gene expression kinetics during FV3 infection

Spleen, peritoneal leukocytes and kidneys were collected from one-year old outbreed *X. laevis* i.p. infected with 1×10^6 PFU of FV3, at the indicated time points ($n = 6$). Gene expression of iVα6-Jα1.43 (*A*, *D* and *G*) or XNC10 (*B*, *E* and *H*) is shown. Results are normalized to an endogenous control and presented as fold change in expression compared with the lowest observed expression of either XNC10 or iVα6. Data are presented as mean ± SE ($n = 6$). FV3 loads were measured using absolute qPCR with primers against FV3 DNA polymerase II (*C*, *F* and *I*). *$P < 0.05$ above bars denotes statistical significance relative to respective uninfected controls and *$P < 0.05$ above the line denote significant differences between the indicated groups (Student *t* test).

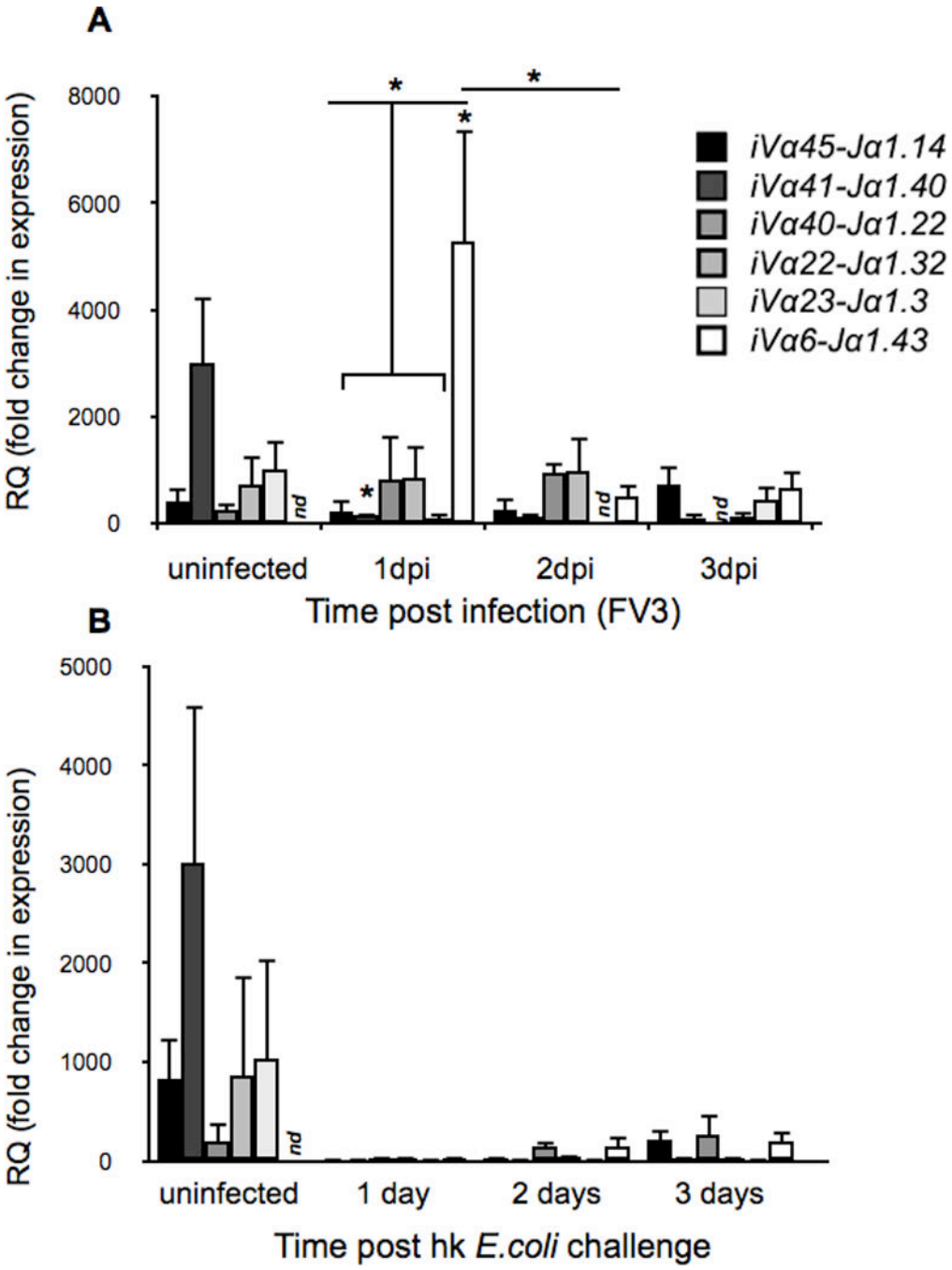

Fig. 3. Relative expression of putative invariant TCRα gene rearrangements in response to FV3 infection and heat killed bacterial challenge

Relative expression of the six predominant invariant TCRα rearrangements (Vα45-Jα1.14, Vα41-Jα1.40, Vα40-Jα1.22, Vα23-Jα1.3Vα22-Jα1.32 and iVα6-Jα1.43) following (A) i.p. FV3 infection (1×10^6 PFU) or (B) intraperitoneal challenge with heat-killed *E.coli*. Results are normalized to an endogenous control and presented as fold change in expression compared with the lowest observed tissue expression. (iVα23 2 days post *E.coli* challenge). All results are presented as mean ± SE (n=5/treatment group), *$P < 0.05$ denotes statistical

significance relative to respective uninfected controls and *$P < 0.05$, when over bars denotes differences between groups denoted by the bars. *nd* = not detected

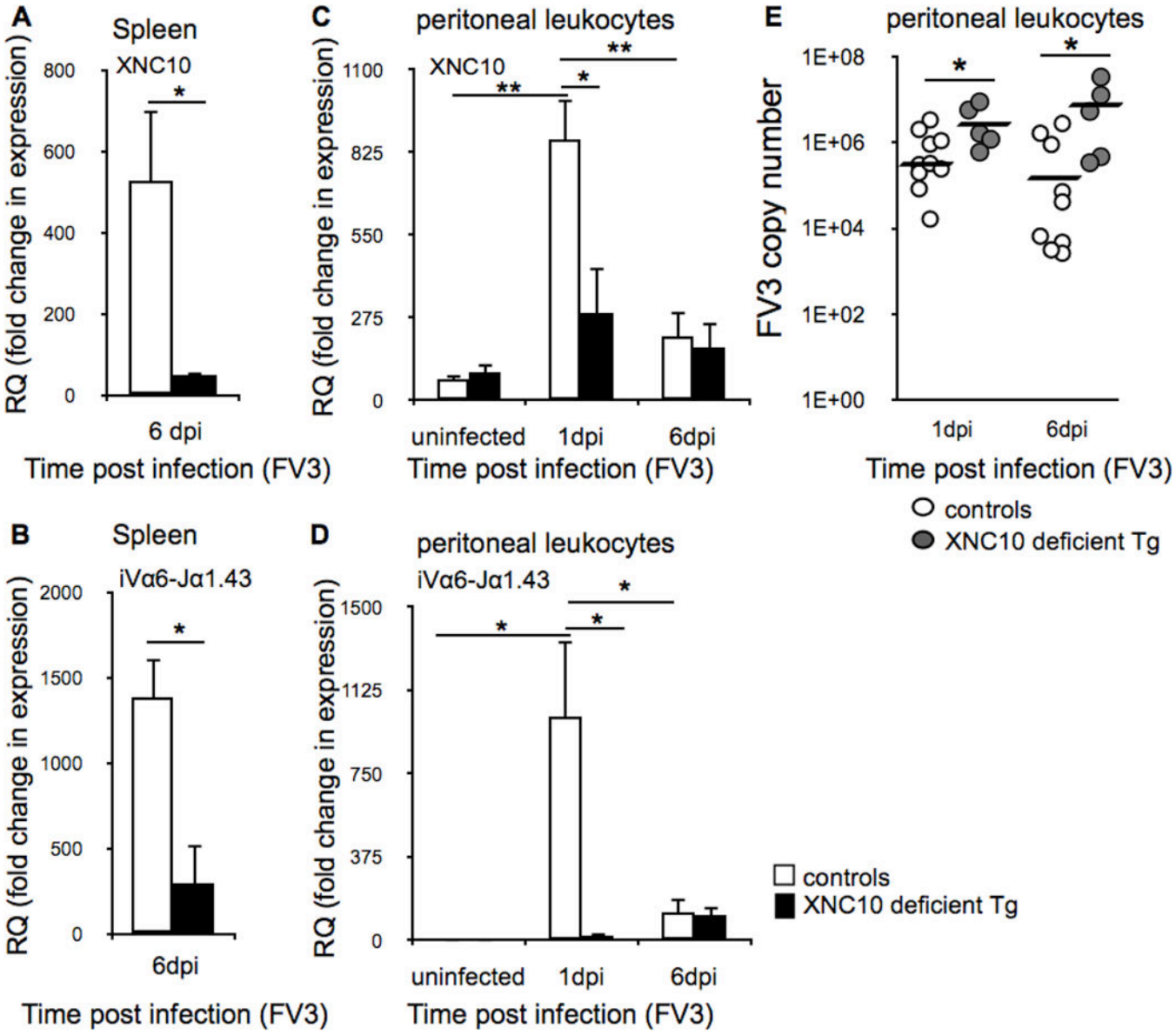

Fig. 4. Impaired control of FV3 replication in peritoneal leukocytes of XNC10-deficient transgenic X. *laevis* lacking iVα6 T cells

One-year old XNC10-deficient transgenic (*n*=5) or age-matched dejellied controls (*n*=8) were i.p. infected with 1×10^6 PFU FV3. XNC10 knock-down was verified by expression of (A) XNC10 and (B) iVα6-Jα1.43 in spleens collected at 6 dpi from XNC10 deficient transgenic (black box) or dejellied controls (white box). Peritoneal leukocytes were collected by peritoneal lavage at 1 and 6 dpi Expression of (C) XNC10 and (D) iVα6-Jα1.43 in XNC10-deficient transgenic adult (black box) or controls (white box). Results are normalized to an endogenous control and presented as fold change in expression compared to the lowest observed expression of XNC10 or iVα6-Jα1.43 respectively and presented as mean ± SE. (E) XNC10-deficient transgenic animals (grey circles, *n*=5) exhibit higher FV3 loads compared to dejellied controls (white circles, *n*=8). Viral loads where assessed by absolute qPCR at 1 and 6 dpi using primers against FV3 DNA polymerase II, $*P < 0.05$ and

**$P < 0.005$ denote significant differences between groups denoted by the bars (Student *t* test).

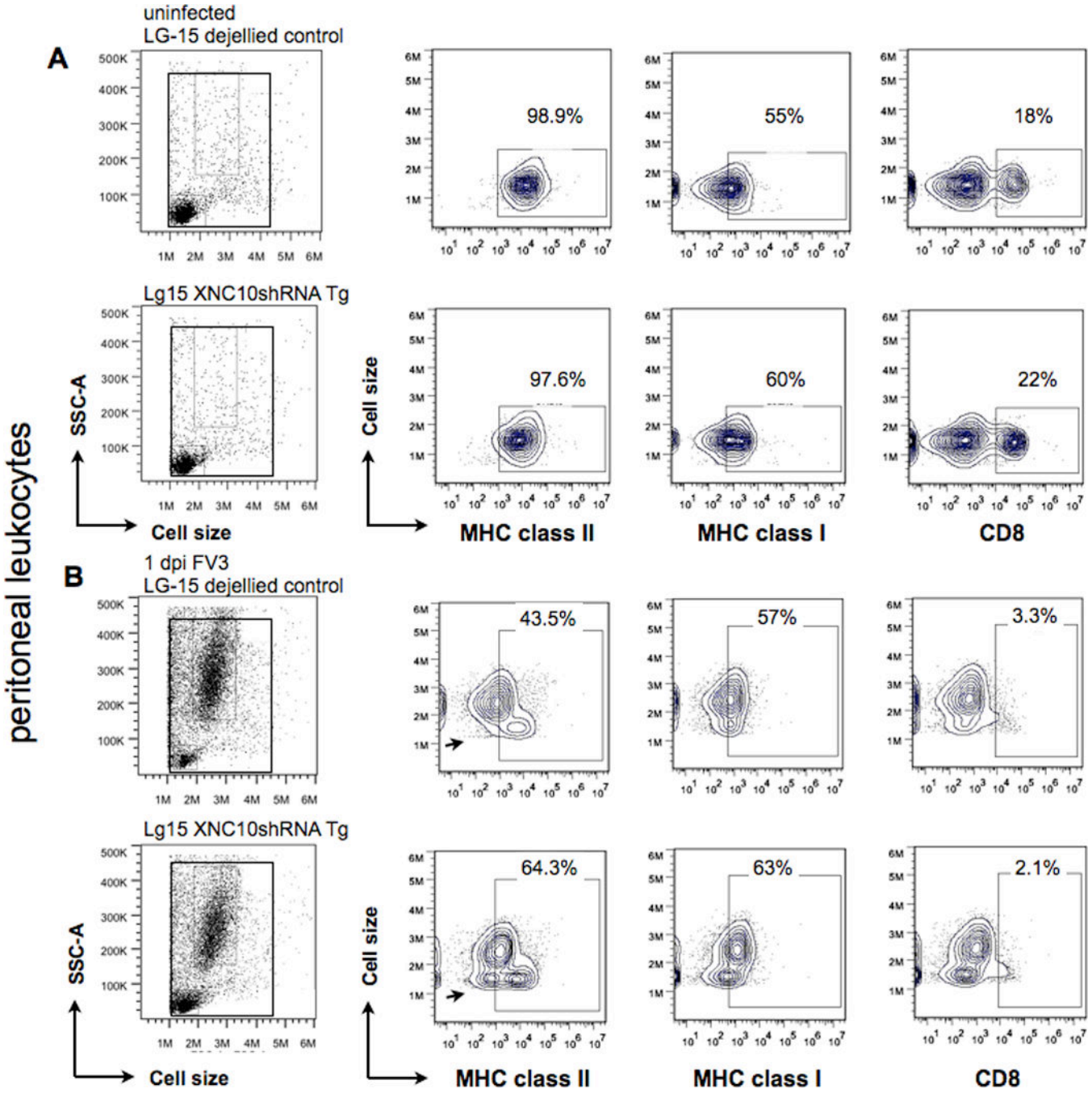

Fig. 5. XNC10-deficiency has little effect on the overall recruitment of MHC class I^+, MHC class II^+ and conventional $CD8^+$ T cells into the peritoneal cavity following FV3 infection

Representative flow cytometry of peritoneal leukocytes isolated from (A) uninfected or (B) FV3 i.p infected (1×10^6 PFU) XNC10-deficient LG-15 transgenic clones and genetically identical non-transgenic LG-15 controls stained with MHC class Ia, MHC class II and CD8-specific mAbs. Scatter profiles and percent positive cells of total live peritoneal are shown. A population of small, agranular MHC class II^{low} staining cells found in FV3 infected XNC10-deficient transgenic is indicated by an arrow.

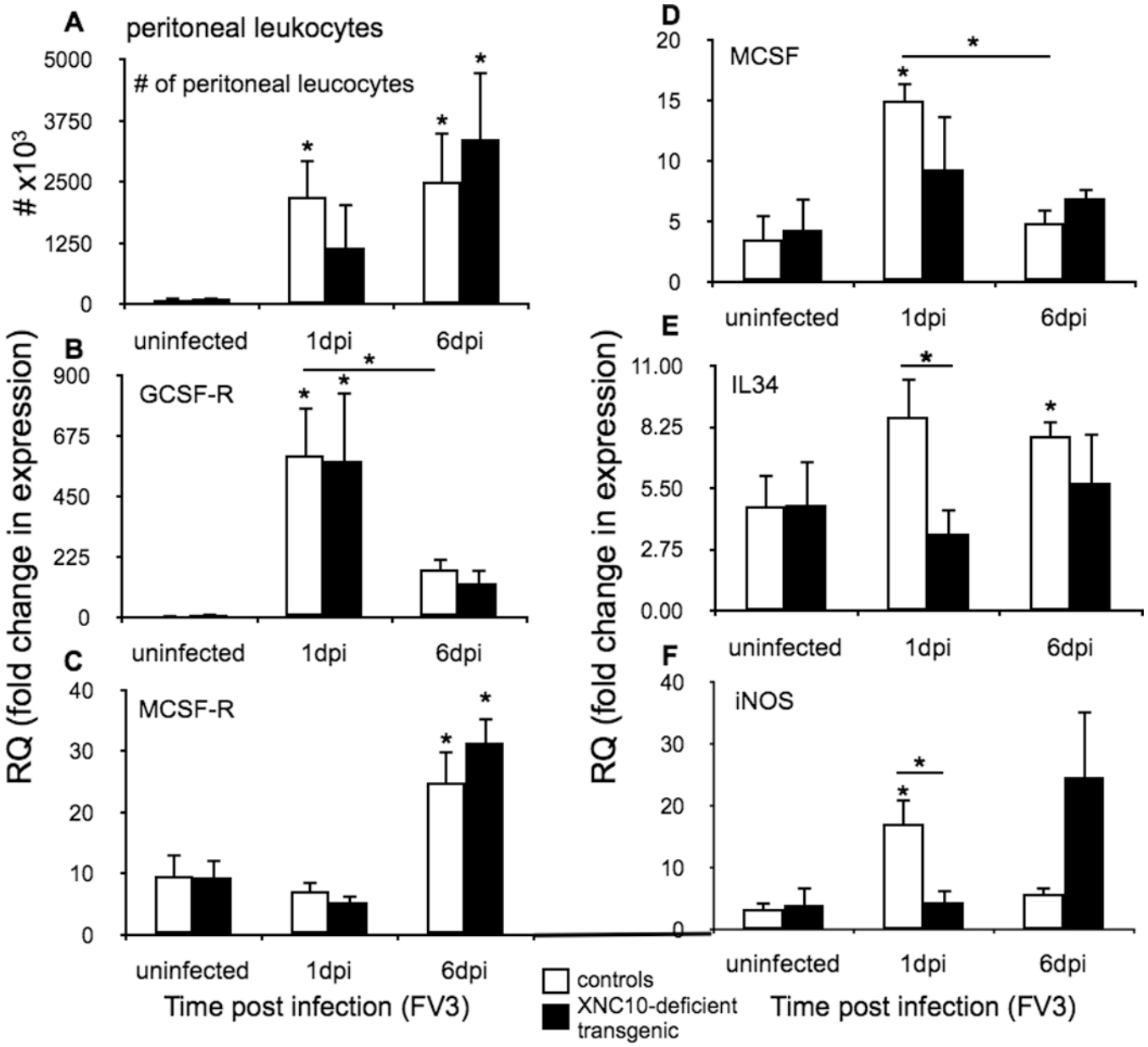

Fig. 6. XNC10 deficiency results in a delayed antiviral peritoneal leukocyte response

One-year old XNC10-deficient transgenic (*n*=5, black box) or age-matched dejellied control (*n*=8, white box) *X. laevis* were i.p. infected with 1×10^6 PFU FV3. (A) Total number of FV3 induced peritoneal leukocytes. Quantitative gene expression analysis of markers for (B) polymorphonuclear monocytes receptors, GCSF-R, (C) macrophage growth factors receptor MCSF-R (D) M-CSF (E) IL-34 and (F) iNOS. Gene expression was determined relative to a endogenous control (GAPDH) and normalized against respective uninfected control gene expression. All results are presented as mean ± SE and $*P < 0.05$ denotes statistical significance relative to respective uninfected controls and $*P < 0.05$, when over bars denotes significant differences between wild-type and XNC10-deficient transgenic groups.

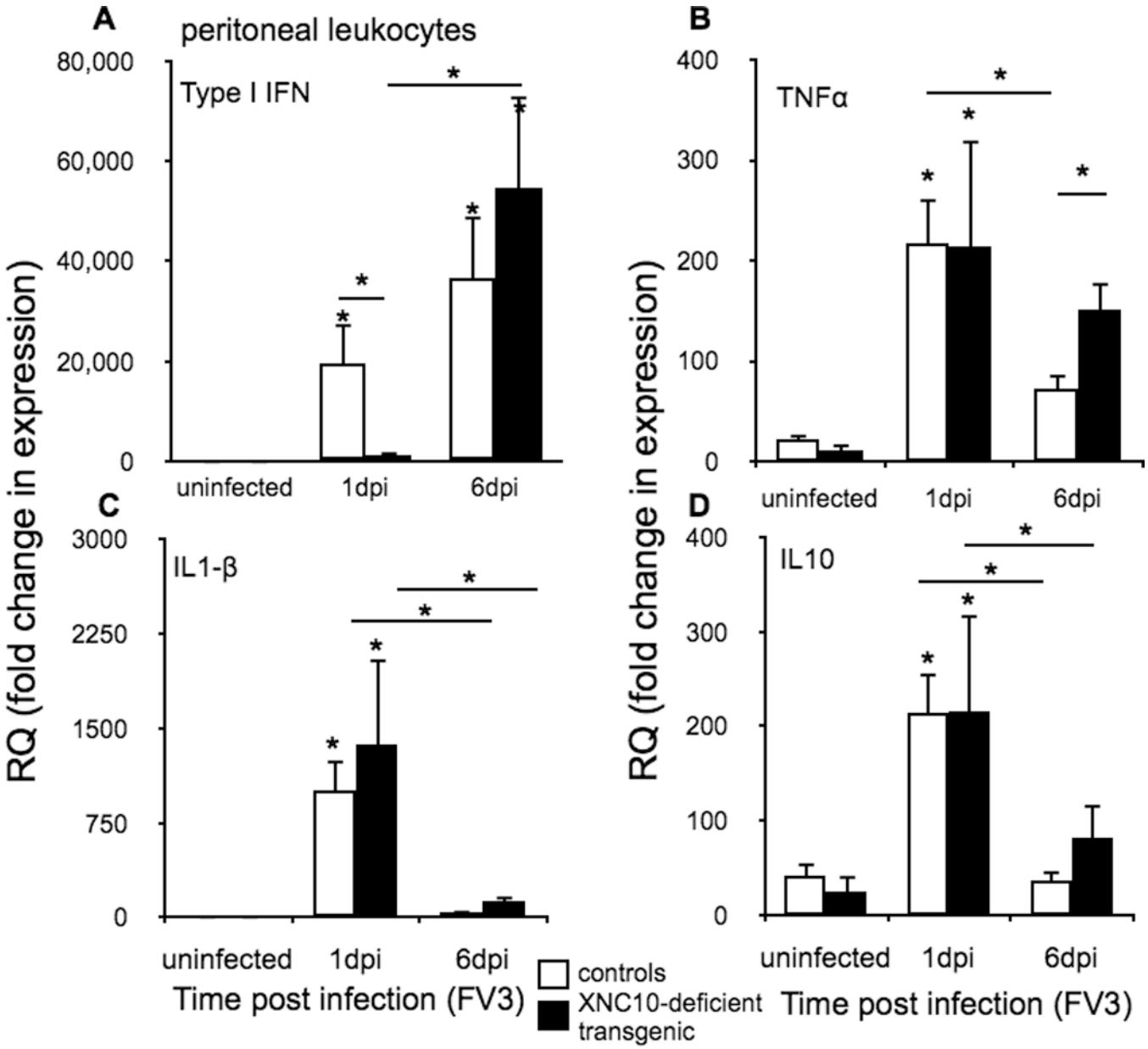

Fig. 7. XNC10-deficient transgenic X. *laevis* have delayed Type I IFN response

Quantitative gene expression analysis of (A) anti-viral (Type I IFN); (B) TNFα (C) IL1-β and (D) IL-10 cytokines in peritoneal leukocytes isolated from either uninfected or FV3 (1×10^6 PFU) infected XNC10-deficient transgenic animals (black box, n=6) or age-matched dejellied control (white box, n=10) at 1 and 6 dpi. Gene expression was determined relative to the endodgenous control GAPDH and normalized against respective uninfected gene expression. All results are presented as mean ± SE and *$P < 0.05$ denotes statistical significance relative to respective uninfected controls and *$P < 0.05$, when over bars denotes significant differences between control and XNC10-deficient transgenic cohorts.

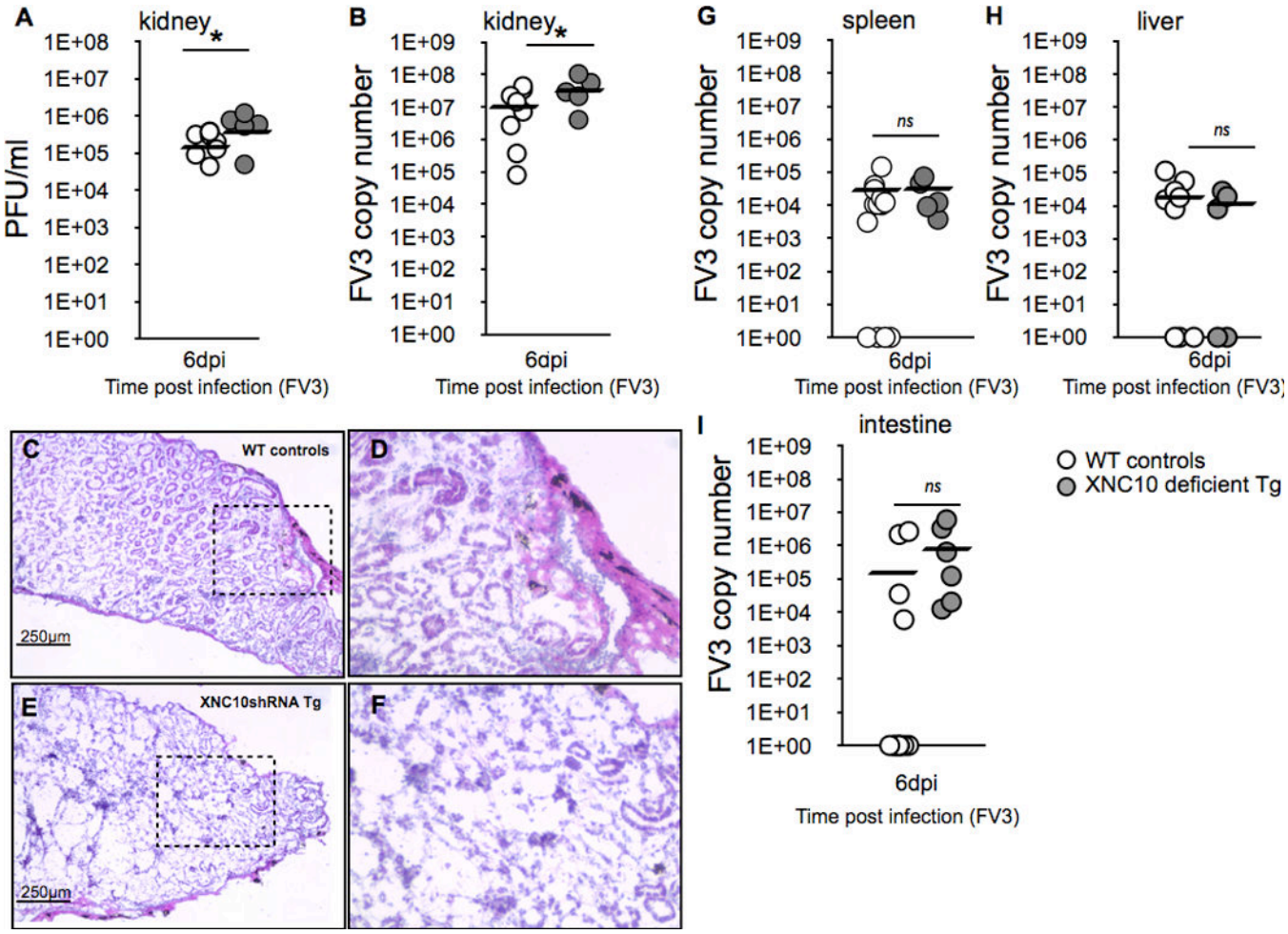

Fig. 8. Increased viral replication and tissue damages in kidneys of transgenic *X. laevis* deficient for XNC10 and iVα6 T cells

One-year old XNC10-deficient transgenic (grey circles, *n*=5) or age-matched dejellied control (white circles, *n*=10) *X. laevis* where i.p. infected with 1×10^6 PFU FV3. Kidneys were collected at 6 dpi and divided into three parts (anterior, middle and posterior) to determine (A; middle part) viral loads by absolute qPCR (viral DNA polymerase II, of 625 ng total DNA) and (B; anterior part) plaque assays. $*P < 0.05$ denotes statistical significance relative to respective uninfected controls and $*P < 0.05$ denote significant differences between groups denoted by the bars (Student *t* test). (C–F; posterior part) Representative histology on cryosections stained with hematoxylin and eosin for (C) controls (D) controls at larger magnification, (E) XNC10-deficient transgenic, (F) XNC10-deficient transgenic, larger magnification. (G–I) XNC10-deficiency has little effect on viral dissemination. Viral loads were assessed at 6 dpi in (G) spleen, (H) liver and (I) intestine by qPCR, *ns* denote no significant differences between groups (Student *t* test).